Primary cilium-mediated MSC mechanotransduction is dependent on Gpr161 regulation of hedgehog signalling

Gillian P. Johnson [a,b,c,d], Sean Fair [d], and David A. Hoey [a,b,c,e]

[a] Trinity Centre for Biomedical Engineering, Trinity Biomedical Sciences Institute, Trinity College, Dublin, D02 R590, Ireland

[b] Dept. of Mechanical, Manufacturing, and Biomedical Engineering, School of Engineering, Trinity College Dublin, Dublin 2, D02 DK07, Ireland

[c] Dept. of Mechanical, Aeronautical and Biomedical Engineering, School of Engineering, University of Limerick, Limerick, V94 PH61, Ireland

[d] Laboratory of Animal Reproduction, Dept. of Biological Sciences, School of Natural Sciences, Faculty of Science and Engineering, University of Limerick, Limerick, V94 T9PX, Ireland

[e] Advanced Materials and Bioengineering Research Centre, Trinity College Dublin & RCSI, Dublin 2, D02 VN51, Ireland

Correspondence

Prof. David A. Hoey, PhD, Dept. of Mechanical and Manufacturing Engineering, School of Engineering, Trinity College Dublin, Dublin 2, D02 DK07, Ireland. Tel: +353 1896 1359, email: dahoey@tcd.ie

Running Title

Gpr161 mediated primary cilia mechanotransduction

Keywords

Bone, Osteogenesis; Oscillatory fluid shear; Mesenchymal Stem/Stromal Cell; G protein coupled receptor

Abstract

The benefits of physical loading to skeletal mass is well known. The primary cilium has emerged as an important organelle in bone mechanobiology/mechanotransduction, particularly in mesenchymal stem/stromal cells, yet the molecular mechanisms of cilium mechanotransduction are poorly understood. In this study, we demonstrate that Gpr161 is a mechanoresponsive GPCR, that localises to the cilium, and is involved in fluid shear-induced cAMP signalling and downstream osteogenesis. This Gpr161-mediated mechanotransduction is dependent on IFT88/cilium and may act through adenylyl cyclase 6 (AC6) to regulate cAMP and MSC osteogenesis. Moreover, we demonstrate that Hh signalling is positively associated with osteogenesis and that Hh gene expression is mechanically regulated and required for loading-induced osteogenic differentiation through a mechanism that involves IFT88, Gpr161, AC6, and cAMP. Therefore, we have delineated a molecular mechanism of MSC mechanotransduction which likely occurs at the cilium, leading to MSC osteogenesis, highlighting novel mechanotherapeutic targets to enhance osteogenesis.

Introduction

The importance of physical loading in regulating skeletal adaptation has long been established (Frost, 1963). Due to the finite lifespan and non-proliferative nature of the bone forming osteoblast (Park *et al.*, 2012), this cell type must be replenished from a progenitor stem/stromal cell population (Chen *et al.*, 2016; Chan *et al.*, 2018). Therefore, it is hypothesised that skeletal mechanoadaptation must require the osteogenic differentiation of lining cells, osteoprogenitors or mesenchymal stem/stromal cells (MSC) (Knight & Hankenson, 2013; Matic *et al.*, 2016). However, the specific mechanism by which these cells sense a mechanical stimulus and translate this into a bone anabolic response is poorly understood. Deciphering the mechanisms of bone cell mechanotransduction may provide novel insight into disease aetiology, in addition to new targets for mechanotherapeutic development to promote bone formation, by mimicking the beneficial effects of loading at a molecular level (Rando & Ambrosio, 2018).

The primary cilium is a solitary cellular appendage that has recently emerged as a critical mediator of bone cell mechanotransduction and bone mechanoadaptation (Hoey *et al.*, 2012; Chen *et al.*, 2016; Johnson *et al.*, 2018). Extending from the surface of the cell into the extracellular space, the cilium is ideally positioned to sense environmental biophysical cues such as oscillatory fluid shear, which can drive osteogenesis (Stavenschi *et al.*, 2017). In particular, we recently demonstrated the primary cilium acts as a cyclic adenosine 3′,5′-monophosphate (cAMP) responsive mechanosensor in bone marrow stem/stromal cells (MSCs), whereby fluid shear activates cAMP signalling and downstream osteogenesis that is intraflagellar transport protein 88 (IFT88)/cilium dependent (Johnson *et al.*, 2018). Ift88 is

65 a tetricopeptide repeat-containing protein and a central part of the Intraflagellar transport (Ift)
66 complex B, which is transported by kinesin in the anterograde direction and is essential for the
67 formation of the primary cilium (Pedersen and Rosenbaum, 2008). Moreover, we demonstrated
68 that that this cAMP and osteogenic response was mediated by adenylyl cyclase 6 (AC6)
69 which is localised to the ciliary microdomain. This *in vitro* study was validated *in vivo* via a
70 Leptin Receptor (LepR) specific knockout of AC6, where *Lepr-cre;tdTomato;AC6*$^{fl/fl}$ animals
71 have an attenuated response to compressive tibia loading, characterized by a deficient load-
72 induced osteogenic response on the endosteal bone surface (Riffault et al., 2020). This study
73 highlighted the contribution of LepR expressing bone marrow stromal cells and specifically
74 AC6 to mechanoadaptation of bone *in vivo*. Although these studies have highlighted a role
75 for the cilium and AC6 in stem/stromal cell mechanotransduction, it is currently unclear how
76 physical manipulation of the cell can lead to downstream MSC osteogenesis in a cilium
77 and/or AC6 dependent manner.

78 Hedgehog (Hh) signalling is an important pathway regulating cell differentiation during
79 development (Shi *et al.*, 2015), critical for limb patterning and skeletal morphogenesis (Ehlen
80 *et al.*, 2006), in addition to regulating adult MSC osteogenic lineage commitment (Spinella-
81 Jaegle *et al.*, 2001; James *et al.*, 2012). Hh signalling is coordinated at the primary cilium,
82 where Smoothened (Smo) activates the Gli transcription factors at the ciliary tip (Berbari *et*
83 *al.*, 2009; Bangs & Anderson, 2017). Anomalies in the Hh pathway trigger skeletal
84 abnormalities similar to that seen in ciliopathies (mutations in genes that encode for IFT)
85 (Ehlen *et al.*, 2006; Ruiz-Perez *et al.*, 2007). Interestingly, cAMP has been highlighted as a
86 regulator of Hh signalling. Despite a number of studies demonstrating a negative association

87 (Vuolo *et al.*, 2015), a positive role for the cAMP pathway in Hh signalling was demonstrated
88 in chick embryos where it is essential for limb development (Tiecke *et al.*, 2007). Moreover,
89 activation of cAMP in mouse embryonic fibroblasts increases Smo trafficking to the cilium
90 activating Hh signalling (Tiecke *et al.*, 2007; Wilson *et al.*, 2009). However, despite the role
91 of Hh signalling in MSC osteogenesis and Hh association with cAMP and the primary cilium,
92 it is currently unclear whether Hh is required for MSC and/or primary cilium
93 mechanotransduction.

94 G protein coupled receptors (GPCRs) constitute one of the most important components of
95 cell signalling cascades, where they are the primary receiver of external stimuli. Upon contact
96 with a ligand, or mechanical stimulus, GPCRs undergo conformational changes thereby
97 activating G proteins by promoting the exchange of GDP/GTP associated with the Gα subunit
98 (Chachisvilis *et al.*, 2006), which results in the transduction of external signals to appropriate
99 downstream effectors. For example, signalling through stimulatory G-proteins ($G_s\alpha$)
100 activates adenylyl cyclase's which in turn initiates cAMP signalling (Chen *et al.*, 1997). The
101 orphan GPCR, GPR161, was recently shown to localize to the primary cilium and regulate
102 Hh signalling via cAMP in mice (Mukhopadhyay *et al.*, 2013). Furthermore, *Gpr161*
103 deficiency in craniofacial mesenchyme prevented intramembranous bone formation in
104 calvarium, and *Gpr161* knockouts were unable to undergo osteoblastic differentiation
105 (Hwang *et al.*, 2018). Given the known role for the Ift88/ciliary localized Gpr161 in Hh
106 signalling, via cAMP, and its critical role in skeletal development, Gpr161 represents a
107 potential important component of MSC osteogenic differentiation and possible key factor in
108 cilium-mediated MSC mechanotransduction.

Therefore, the aim of this study was to delineate the molecular components of Ift88/cilia-mediated-MSC mechanotransduction leading to osteogenesis; the identification of which could lead to new mechanotherapeutics to enhance bone regeneration. Here, we demonstrate that Hh signalling is positively associated with osteogenesis and demonstrate that Hh signalling is mechanically regulated and required for loading-induced MSC osteogenic differentiation. Moreover, using *Ift88* and *AC6* siRNA we identified that fluid shear activated Hh and osteogenic signalling is dependent on *Ift88*/primary cilium and ciliary localised AC6, through their control of the cAMP second messenger. Importantly, we have also identified an upstream component of cilium-mediated mechanotransduction in the form of the orphan GPCR, Gpr161, which localises to the primary cilium. We also demonstrate, for the first time, that Gpr161 is mechanoregulatory mediating loading-induced cAMP, hedgehog, and osteogenic gene expression, therefore highlighting a novel mechanosensitive GPCR. Therefore, we have delineated a molecular mechanism of MSC mechanotransduction which occurs at the primary cilium, whereby a biophysical stimulus triggers a pathway that involves Gpr161, AC6, cAMP, and Hh leading to MSC osteogenesis.

Materials and Methods

Cell Culture

The murine mesenchymal stem/stromal cell line C3H10T1/2 was obtained from ATCC (LGC Standards, Teddington, Middlesex, UK). MSCs were tested to confirm lack of mycoplasma contamination MycoAlert PLUS detection kit (LT07, Brennan &Co). MSCs were maintained in Dulbecco's modified Eagle's medium (DMEM; D6046, Sigma-Aldrich, St Louis, MO,

USA) with low glucose (Sigma-Aldrich, St Louis, MO, USA) supplemented with 10% fetal bovine serum (FBS; South American origin, Labtech International, Ltd. Heathfield, East Sussex, UK) and 1% Penicillin Streptomycin (P/S; P4333, Sigma Aldrich, St Louis, MO, USA). Cells were only used for experiments when they had reached 80% confluency and were at a passage between 12-17.

Biochemical modulation of Hedgehog Signalling

Hh signalling was modulated by means of cyclopamine treatment (sc-200929; Santa Cruz Biotechnology, Inc., Dallas, Texas, U.S.A). Cyclopamine is a plant derived pathway antagonist that acts at the level of Smo and thus over short term treatment is known to inhibit Hh signalling. However, long term treatment can result in Hh activation due to corrective feedback loop (Alcedo *et al.*, 2000). Dose and time response studies were performed to determine the optimum concentration and duration of treatment of cyclopamine that effectively inhibited Hh signalling. The optimal dose and time combination of 1μM and 6 hrs was chosen for further studies investigating the effect of Hh inhibition on OFS changes in Hh and osteogenic gene expression. Controls were incubated for the same duration of time with vehicle (Ethanol;0.02%) treated medium for both dose response and OFS studies.

Biochemical Inhibition of cAMP Signalling

Cyclic AMP signalling was diminished through the inhibition of adenylyl cyclase activity by MDL-12,330A hydrochloride as previously described (MDL; M182; Sigma-Aldrich, (Johnson *et al.*, 2018)). MSCs were treated with MDL supplemented medium throughout application of the 1Pa mechanical stimulation, and controls were incubated for the same time frame with vehicle (H_2O) treated medium.

Ift88/Primary cilium, *Ac6* and *Gpr161* Knockdown

Intraflagellar transport protein 88 (*Ift88*), *Ac6* and *Gpr161* were inhibited by siRNA. Lipofectamine RNAiMAX (Invitrogen) was diluted 1/135 in OptiMEM reduced serum transfection medium (Gibco, Foster City, CA, USA). For *Ift88* knockdown this was mixed 1:1 with predesigned Stealth RNAi targeting *Ift88* (MSS211714, Invitrogen) at a dilution of 16.7µM in OptiMEM and incubated at room temperature for 15 min before application, while for *Ac6* and *Gpr161* knockdown lipofectamine was mixed 1:1 with Silencer Select Ambion small-interfering RNA (siRNA; 4390825, AM16704; Bio-Sciences Limited, Dublin, Ireland) at a dilution of 60pmol for 5 min before adding 600µl of the reaction mix to cells and incubating for 8 hours at 37°C, following which 10 ml DMEM (0.5% FBS, 1% P/S) was added to the cells for 24h. The off-target control was Stealth RNAi Negative Control, Medium GC (12935300, Invitrogen) and Silencer™ Negative Control (AM4641, Thermo-Fisher), respectively. Forty-eight hours following transfection the transfected cells were seeded for experimentation in DMEM (0.5% FBS, 1% P/S). Transfection efficiency was verified 72 hrs after transfection by qRT-PCR and immunocytochemistry as described above.

Mechanical Stimulation

MSCs were seeded on fibronectin (10 µg/ml) coated glass slides and oscillatory fluid flow induced shear stress was applied to MSCs with the use of in-house custom designed parallel plate flow chambers (Stavenschi *et al.*, 2017). Oscillatory fluid shear (OFS) of 1Pa was applied to cells at 1Hz frequency for 2 hrs for gene expression studies and 15 mins for cAMP studies. The no flow controls take account of the confined environment experienced by cells within the chambers. They consist of cell seeded glass slides prepared in the same way, where

slides were placed within the chambers for 2 hrs or 15 mins but are not attached to the syringe pump.

Quantitative Real-Time Polymerase Chain Reaction (qRT-PCR)

Immediately after treatment, cells were lysed with TRI Reagent® (93289; Sigma Aldrich, St Louis, MO, USA), and mRNA was extracted as per the manufacturer's protocol. The concentration of RNA in each sample was measured using a Nanodrop spectrophotometer and 400ng of RNA was reverse transcribed to cDNA using the High-Capacity cDNA Reverse Transcription Kit (Applied Biosystems, Foster City, CA, USA). The expression of ribosomal RNA 18s (*18s*), Protein patched homolog 1 (*Ptch1*), Zinc finger protein GLI1 (*Gli1*), runt-related transcription factor 2 (*Runx2*), Osteopontin (*Opn*), and G Protein-Coupled Receptor 161 (*Gpr161*) were amplified for analysis following treatments with cyclopamine, oscillatory fluid shear, and MDL-12,330A hydrochloride. Validation of transient siRNA knockdowns (Sigma Aldrich, St Louis, MO, USA) was also assessed by mRNA expression. Quantitative RT-PCR (qRT-PCR) was performed using a 20 µl reaction mix containing 10 µl SYBR green PCR MasterMix (Invitrogen Ltd, Paisley, UK), 0.8 µl of each primer, and 8.4 µl of sample and H_2O mix. In the case of *Runx2, Ac6* and *Gpr161* 0.6 µl of each primer was used, where an additional 0.4 µl H_2O was added to maintain the final volume of 20 µl. Plates were run in an ABI 7500 Fast Real-Time PCR machine (Life Technologies, Carlsbad, CA, USA). The cycle parameters were as follows: Uracil N-glycosylase (UNG) activation was run for 2 min at 50°C, DNA polymerase activation for 10 min at 95°C, the melt cycle was run for 15s at 95°C and the annealing–extending cycle for 1 min at 60°C for *Ptch1*, *Gli1*, *Runx2*, *Opn, Ift88* and *Gpr161*, apart from *18s* and *Ac6* which was run at 65°C. A no-template control (NTC)

was run in each 96-well plate to confirm the absence of contamination. Each sample was normalized to reference gene 18S and to static or no treatment control using relative quantification method. All primer sequences and concentrations are outlined in Table S1.

Quantification of cAMP signalling

Cyclic AMP activity was analysed using the commercially available Cyclic AMP XP® Assay Kit (Cell signaling technology, Danvers, MA, USA). Cells were rinsed with ice cold phosphate buffered saline following OFS (PBS; Sigma Aldrich, St Louis, MO, USA) and lysed on ice with 200µl RLT lysis buffer containing phenylmethylsulfonyl fluoride (PMSF; 1:200; Sigma Aldrich, St Louis, MO, USA). Experimental samples (50 µl) were loaded into the anti-cAMP XP® rabbit mAb coated plate, with 50 µl HRP-linked cAMP solution and incubated on an orbital plate shaker for 3 hrs at room temperature (RT). Wells were washed with 200 µl 1X wash buffer four times, before incubating with 100 µl 3,3',5,5'-Tetramethylbenzidine (TMB) substrate for 30 min at RT. Following 30 min, 100 µl stop solution was added. Plate absorbance was read at 450 nm. All samples including the standard curve were run in triplicate. Media was supplemented with 1µM 3-Isobutyl-1-methylxanthine (IBMX) for all cAMP studies.

Immunocytochemistry

MSCs were seeded on fibronectin coated glass coverslips for 24 hours before serum starvation in DMEM low glucose, 0.5% FBS, 1% P/S for 48 hours. After fixation in neutral buffered formalin for 10 min (Sigma Aldrich, St Louis, MO, USA), coverslips were permeabilized in 0.1% Triton X-100 and non-specific binding sites were blocked using 1% w/v BSA (Sigma Aldrich, St Louis, MO, USA) in PBS for 2 hrs at room temperature. Primary

antibody targeting the primary cilium (anti-acetylated α-tubulin, ab24610, Abcam, Cambridge, UK) was applied at 1:1500 overnight at 4°C. Next the primary antibody for centrioles (anti-pericentrin, ab4448, Abcam, Cambridge, United Kingdom) was used at a dilution of 1:1500 for 1h at RT to clearly identify the base of the cilium. The secondary antibodies AlexaFluor 594 and AlexaFluor 488 (A21203, A21202; Life Technologies, California, USA) were applied in tandem at 1:500 for 1h at room temperature in the dark. For validation of AC6 knockdown, the primary antibody targeting AC6 (anti-AC6, ab14781, Abcam) was applied for 1 h at room temperature at a dilution of 1:500. the secondary antibody AlexaFluor 488 (A21202; Life Technologies, California, USA) was applied at 1:500 for 1h at room temperature in the dark. For GPR161 expression and spatial organization, the primary antibody targeting GPR161 (ab58679; Abcam, Cambridge, United Kingdom) was applied for 1h at room temperature at a dilution of 1:200 followed by AlexaFluor 488 secondary antibody (A21202; Life Technologies, California, USA) for 1h at room temperature at 1:500. Finally, DAPI at 1:2000 in PBS (32670; Sigma-Aldrich) was applied to all samples for 5 min prior to sample mounting on glass slides using Prolong gold mounting medium (P36934; Invitrogen). Imaging was performed on the Leica SP7 (Leica Microsystems, Wetzlar, Germany) scanning confocal microscope at 63x (N.A. 1.40 Oil). Controls in the absence of primary antibody were used to test for non-specific binding and background staining of the secondary antibodies.

Data/Statistical Analysis

The relative expression of each gene with reference to *18s* was calculated and the results expressed as fold change in gene expression relative to the no flow scrambled or vehicle

control group along with the standard deviation. For the cyclopamine, OFS, MDL treated, *Ac6*, *Ift88* and *Gpr161* knockdown studies a two-way ANOVA analysis was performed with Bonferroni correction post-hoc tests. Mechanical regulation of *Gpr161*, *Gpr161* expression post *Ift88* knockdown and validation of *Gpr161* knockdown studies were analysed using two-tailed unpaired student's t-test with Wilcoxon correction. All data were analysed using Graph Pad Prism 8. Only primers with PCR efficiencies between 90% and 110% were used. In all experiments, $p<0.05$ was considered statistically significant. Technical replicates are represented as N, while biological replicates are represented as n.

Results

Hedgehog inducible gene expression is positively associated with MSC osteogenesis

To determine if Hh induced gene expression is associated with MSC osteogenesis, we quantified hedgehog and osteogenic gene expression following treatment with Hh antagonist cyclopamine. Firstly, we performed a dose response study where cells were treated with either vehicle control (ethanol;0.02%), 1-, 5-, or 10 μM cyclopamine for 6, 12, or 24 h to determine the optimum concentration and time of cyclopamine treatment that inhibits Hh signalling as determined by *Ptch1* and *Gli1* gene expression ($p<0.05$, Fig. 1A-D). We found that all three concentrations of cyclopamine reduce hedgehog gene expression at 6 hrs (*Ptch1* and *Gli1*; $p<0.05$; Fig. 1A-B). However, 1- and 5 μM increased Hh genes at 12 hrs ($p<0.001$; Fig. 1A-B), while 10 μM did not have a significant effect at the later timepoints, suggestive of a biphasic effect of cyclopamine and presence of a Hh regulatory feedback loop, as has been shown before (Alcedo *et al.*, 2000).

263 Interestingly, the trends seen in Hh induced gene expression following cyclopamine
264 treatment very closely mirror that seen in osteogenic gene expression. At 6 hrs treatment, all
265 three concentrations of cyclopamine reduced osteogenic gene expression (*Runx2* and *Opn*;
266 $p<0.05$; Fig. 1C-D). However, at 12 hrs, 1- and 5 μM increased osteogenesis significantly
267 (*Runx2* and *Opn*; $p<0.01$; Fig. 1C-D). The similar trends seen between Hh activity and
268 osteogenesis indicate a strong positive relationship in MSCs.

269 In order to study the effect of Hh induced gene expression on downstream osteogenesis, a
270 concentration of 1 μM at 6 h was chosen for all further studies, as it was the lowest
271 concentration and shortest treatment time which resulted in an inhibition of all Hh associated
272 genes analysed.

273 **Hedgehog** induced gene expression **is mechanoresponsive and is required for fluid shear-**
274 **induced osteogenesis in MSCs**

275 Given the demonstrated association between changes in Hh gene expression and osteogenesis
276 and known role for mechanical loading in driving MSC osteogenic differentiation
277 (Stavenschi *et al.*, 2017; Stavenschi *et al.*, 2018), we next sought to determine whether Hh
278 signalling was mechanoresponsive and involved in loading-induced osteogenesis. To
279 determine if Hh induced gene expression is mechanoresponsive in MSCs, we quantified Hh
280 gene expression following 2 hrs of OFS. *Ptch1* and *Gli1* expression were significantly
281 upregulated 3.6-fold and 3.3-fold respectively when compared to static controls ($p<0.05$; Fig.
282 2 A-B), demonstrating that Hh induced gene expression is mechanically regulated. To
283 determine whether this Hh induced gene expression is required for downstream osteogenesis,
284 we treated MSCs with cyclopamine as previously described. As expected cyclopamine

285 resulted in a decrease in basal Hh gene expression but importantly inhibits the increase in Hh
286 signalling seen with mechanical loading.
287 The application of 2 hrs OFS significantly upregulates osteogenic genes *Runx2* and *Opn* 3.1-
288 fold and 5-fold respectively ($p<0.01$; Fig. 2C-D), which is consistent with our previous
289 findings (Johnson *et al.*, 2018). However, following inhibition of the mechano-activation of
290 Hh induced gene expression via cyclopamine treatment, the increase in MSC osteogenesis is
291 lost, demonstrating that Hh induced gene expression is an important pathway in loading-
292 induced MSC osteogenesis.

293 **Fluid shear-induced hedgehog and osteogenic signalling in MSCs is dependent on**
294 ***Ift88*/primary cilia**

295 The primary cilium has previously been shown to be required for MSC mechanotransduction,
296 specifically with regards to fluid shear-induced increases in osteogenic gene expression
297 (Hoey *et al.*, 2012). Furthermore, the cilium has long been associated with Hh signalling
298 (Bangs & Anderson, 2017). Therefore, we next sought to determine whether the cilium was
299 required for mechanically mediated Hh and osteogenic gene expression. The formation of
300 primary cilia was inhibited through the utilization of siRNA targeting *Ift88*, which is a
301 principal motor protein required for ciliogenesis. Primary cilia were identified in the
302 perinuclear region of the cell (Fig. 3A). This transfection procedure resulted in a significantly
303 diminished *Ift88* mRNA expression ($p<0.05$, Fig. 3C), leading to a 70% reduction in the
304 incidence of primary cilia as demonstrated by immunocytochemistry ($p<0.001$, Fig. 3A–B,
305 D). Moreover, the remaining cilium were reduced in length suggestive of defective IFT
306 ($p<0.01$; Fig 3C-E).

Scrambled siRNA transfection did not affect the Hh response to fluid shear, with significant 2.8-fold increases in *Ptch1* and 2.8-fold increase in *Gli1* ($P<0.05$; Fig. 3F-G). However, depletion of the primary cilium via *Ift88* knockdown resulted in a highly variable response, where no change was found in basal Hh levels. In MSCs which have absent or defective IFT/primary cilia, the fluid shear-induced activation of Hh is lost, demonstrating an important role for the primary cilium in mechanically-activated Hh signalling. Similarly, with regards to osteogenic gene expression, scrambled siRNA transfection did not affect the osteogenic response to fluid shear, with significant 3.2-fold increases in *Runx2* and 2.9-fold increase in *Opn* ($P<0.05$; Fig. 3H-I), nor did primary cilia depletion via *Ift88* knockdown affect basal osteogenic gene expression. Yet, treatment with *Ift88* siRNA resulted in a loss of the fluid shear-induced increase in osteogenic gene expression, which is consistent with previous findings. Taken together, this data demonstrates that the primary cilium is required for fluid shear induced hedgehog signalling and downstream MSC osteogenesis.

Primary cilium localized adenylyl cyclase 6 (AC6) is required for fluid shear-induced hedgehog gene expression in MSCs

As adenylyl cyclase's have a demonstrated role in OFS-induced osteogenesis in MSCs via regulation of the second messenger cAMP (Johnson *et al.*, 2018), we endeavoured to further investigate the role of ACs in hedgehog dependent osteogenesis. AC activity was inhibited by MDL-12,330A hydrochloride (MDL) treatment, as previously described (Johnson *et al.*, 2018) and MSCs were subjected to OFS at 1Pa, 1Hz for 2h. Expression of *Ptch1* and *Gli1* in vehicle treated MSCs exposed to OFS increased by 3.3- and 8.8-fold respectively ($P<0.05$; Fig. 4A-B), however, this response was lost in MSCs treated with MDL, demonstrating that mechanical activation of Hh signalling is AC and subsequently cAMP dependent.

We have previously demonstrated that this cAMP dependent mechanotransduction mechanism, was mediated by the specific adenylyl cyclase, AC6, which co-localises to the primary cilium (Johnson *et al.*, 2018). Therefore, to investigate the role of AC6 specifically in loading-induced Hh signalling, we depleted *Ac6* in MSCs using siRNA, as verified by immunocytochemistry (Fig. 4C-D) and qPCR (Fig. 4E). *Ac6* mRNA levels were diminished by 44% in AC6 siRNA treated cells (Fig. 4E). AC6 is located across the cell membrane but is concentrated along the ciliary axoneme (Fig. 4C), in close contact with the hedgehog signalling components known to localise to the ciliary microdomain (Goetz *et al.*, 2009). No staining was found when AC6 primary antibody was withheld (Fig. S1). MSCs were treated with either off-target scrambled or *Ac6* targeting siRNA and were subjected to 2 hrs of OFS to assess the role of AC6 in OFS-induced expression of *Ptch1* and *Gli1*. Hedgehog genes in the no flow group were unaffected by the *Ac6* siRNA treatment, demonstrating that AC6 activity does not influence basal hedgehog signalling. When exposed to fluid shear, MSCs treated with scrambled siRNA exhibited a 6.9- and 3.7-fold increase in *Ptch1* and *Gli1* gene expression, respectively ($P<0.01$; Fig. 4F-G), demonstrating no effect of the transfection treatment. However, upon depletion of *Ac6* no change in hedgehog gene expression was found in MSCs following oscillatory fluid shear (Fig. 4F-G), demonstrating the specific role of AC6 in regulating mechanically activated hedgehog signalling.

Gpr161 is expressed by MSCs, localizes to the primary cilium, and is mechanically regulated upstream of AC6

The orphan G-protein coupled receptor 161 (Gpr161) is known to localize to the cilium and be involved in the regulation of hedgehog signalling in the neural tube (Mukhopadhyay *et*

352 *al.*, 2013). Importantly Gpr161 also regulates forelimb formation, limb patterning and
353 skeletal morphogenesis in a primary cilium-dependent manner (Hwang *et al.*, 2018). To
354 investigate the potential role of Gpr161 in cilium-mediated MSC mechanotransduction, we
355 first determined the expression and spatial organization of Gpr161 in MSCs using
356 immunocytochemistry. Gpr161 is expressed across the MSC cell membrane (Fig. 5A) and
357 interestingly upon co-staining for acetylated α-tubulin, a distinct spatial organization was
358 revealed within the primary cilium, with intense staining identified along the ciliary axoneme
359 (Fig. 5A). No staining was found when GPR161 primary antibody was withheld (Fig. S2).
360 Being an orphan GPCR, the ligand for Gpr161 is unknown, however a number of GPCR are
361 mechanoresponsive (Xu *et al.*, 2018). To determine whether this is the case for orphan Gpr161,
362 MSCs were subjected to 1Pa, 1Hz OFS for 2hrs and it was revealed that *Gpr161* mRNA levels
363 significantly increased 2.7-fold following exposure ($P<0.01$; Fig. 5B), demonstrating the
364 mechanoresponsive nature of this GPCR. Interestingly, depletion of the primary cilium via
365 *Ift88* knockdown significantly reduced *Gpr161* expression ($P<0.05$; Fig. 5C), and *Gpr161* gene
366 expression failed to increase following OFS in MSCs treated with *Ift88* siRNA (Fig. 5D),
367 indicating the cilium is an important regulator of this receptor. As cilia-localised Gpr161 has
368 been previously shown to couple to stimulatory $G_s\alpha$ to activate ACs and produce cAMP
369 (Mukhopadhyay *et al.*, 2013), we next sought to investigate whether AC6 is involved in
370 Gpr161 mechanoregulation. Transient deletion of *Ac6* via siRNA in MSCs had no effect on
371 either basal, nor OFS-induced expression of *Gpr161*, indicating that AC6 is not a direct
372 regulator of Gpr161 and likely acts downstream in MSC mechanotransduction ($P<0.05$; Fig.
373 5E).

Gpr161 is required for fluid shear-induced cAMP second messenger signalling in MSCs

As we have previously demonstrated that *Ift88*/primary cilium acts as a cAMP responsive mechanosensor in MSCs (Johnson *et al.*, 2018) and given the spatial organization of Gpr161 at the primary cilium, we next examined whether Gpr161 is responsible for the flow-mediated changes in cAMP signalling. To investigate the role of Gpr161 in cAMP signalling, *Gpr161* was depleted in MSCs using siRNA targeting *Gpr161*. Gpr161 was found to be abundant and localize to the cilium in cells treated with scrambled siRNA (Fig. 6A), while treatment of *Gpr161* siRNA resulted in a near complete loss of Gpr161 protein expression as verified by immunocytochemistry (Fig. 6B). Furthermore, *Gpr161* mRNA levels decreased by 60% compared to scrambled control following siRNA treatment ($P<0.001$; Fig. 6C). MSCs treated with either scrambled or *Gpr161* siRNA were subjected to 15 min of OFS to assess cAMP signalling (Fig. 6D). OFS increased cAMP levels within the cell 3.21-fold compared to no flow controls in cells treated with scrambled siRNA ($P<0.05$; Fig. 6D), which is consistent with previous findings (Johnson *et al.*, 2018) and demonstrates no effect of scrambled treatment on MSC behaviour. However, MSCs deficient in Gpr161 do not respond to OFS with an activation of cAMP signalling (Fig. 6D), indicating that *Gpr161* is required by MSCs in mechanically mediated cAMP second messenger signalling, potentially via AC6.

Fluid flow-induced increases in hedgehog and osteogenic signalling is dependent on *Gpr161* in MSCs

Finally, we wanted to investigate whether Gpr161 plays a role in OFS-induced increases in hedgehog and osteogenic signalling, which we had previously shown is dependent on *Ift88*/cilia. Firstly, to analyse Hh signalling, both scrambled and *Gpr161* siRNA treated MSCs

were subjected to 2 hrs of OFS and expression of *Ptch1* and *Gli1* were analysed. In the scrambled control MSCs, expression of *Ptch1* and *Gli1* increased 2.8- and 3.4- fold respectively, compared to no flow controls ($P<0.05$; Fig. 7A-B). However, similar to that seen with cAMP signalling, depletion of *Gpr161* resulted in a complete loss of the fluid shear-induced increases in hedgehog gene expression (Fig. 7A-B), indicating that *Gpr161* is a critical component of hedgehog activation through the regulation of cAMP second messenger signalling.

Secondly, to determine whether Gpr161 was required for loading-induced osteogenesis, MSCs treated with either scrambled or *Gpr161* siRNA were subjected to OFS for 2h, following which expression of *Runx2* and *Opn* were analysed. MSCs treated with scrambled siRNA and exposed to fluid shear resulted in significant 5.35- and 4.7-fold increases in *Runx2* and *Opn* mRNA levels, respectively, compared to no-flow controls ($P<0.05$; Fig. 7C-D). Moreover, similar to that seen with cAMP and Hh signalling, depletion of *Gpr161* resulted in a loss of the fluid shear-induced increases in osteogenic gene expression (Fig. 7C-D), demonstrating that Gpr161 is a critical component of MSC mechanotransduction. Schematic of proposed molecular mechanism of cilia mediated mechanotransduction in MSCs is depicted in (Fig. 8).

Discussion

The benefits of physical loading to skeletal mass and architecture is well known, yet the mechanisms mediating mechanoadaptation are poorly understood. We and others have

417 recently demonstrated a significant role for the primary cilium in bone mechanobiology and
418 mechanotransduction, particularly in mesenchymal stem/stromal cells (Hoey *et al.*, 2012;
419 Chen *et al.*, 2016; Labour *et al.*, 2016; Corrigan *et al.*, 2018; Johnson *et al.*, 2018). Although
420 the cilium can be targeted directly to module MSC mechanosensitivity and osteogenesis
421 (Corrigan *et al.*, 2019), understanding the molecular components of cilium-mediated MSC
422 mechanotransduction may reveal new insights to bone pathologies and identify more
423 effective therapeutic targets to treat bone loss diseases such as osteoporosis. In this study, we
424 demonstrate that Gpr161 is a mechanoresponsive GPCR, that localises to the primary cilium,
425 and is required for fluid shear induced cAMP signalling and downstream osteogenesis. This
426 Gpr161 mediated mechanotransduction is dependent on the IFT88/primary cilium and may
427 act through AC6 to regulate cAMP and MSC osteogenesis. Moreover, we demonstrate that
428 Hh signalling is positively associated with osteogenesis and demonstrate that Hh signalling
429 is mechanically regulated and required for loading-induced MSC osteogenic differentiation
430 potentially through a mechanism that involves IFT88, Gpr161, AC6, and cAMP. Therefore,
431 we have delineated a molecular mechanism of MSC mechanotransduction which likely
432 occurs at the primary cilium, whereby a biophysical stimulus triggers a pathway involving
433 IFT88, Gpr161, AC6, and cAMP leading to MSC osteogenesis, highlighting novel
434 therapeutic targets to enhance MSC osteogenesis, mimicking mechanotransduction at a
435 molecular level.

436 Hedgehog activity is positively associated with osteogenic signalling, is
437 mechanoresponsive, and required for loading-induced increases in MSC osteogenesis. The
438 correlation between Hh activation and osteogenic gene expression demonstrated here is
439 consistent with previous findings in rodent bone marrow MSCs, where treatment with N-

terminal Sonic Hh (Shh) increases the percentage of cells responding positively to bone morphogenetic protein 2 (BMP2), in terms of alkaline phosphatase production, proliferation and osteogenic differentiation (Kinto *et al.*, 1997; Spinella-Jaegle *et al.*, 2001; Cai *et al.*, 2012; Chen *et al.*, 2016c). Moreover, these studies found decreased adipocyte differentiation, highlighting the potential for Hh agonists to constitute novel therapeutics for preventing osteopenic disorders. Interestingly, Hh signalling is activated in response to fluid shear and is required for downstream osteogenesis in MSCs, identifying a key pathway in MSC mechanotransduction. Hedgehog signalling in chondrocytes has been shown to be mechanoresponsive to cyclic tensile strain and hydrostatic pressure where application of both stimuli increased Hh gene expression, and transcription of *Ptch1* and *Gli1* genes (Shao *et al.*, 2012; Thompson *et al.*, 2014). Similarly, our lab has previously shown that both cyclic hydrostatic pressure and oscillatory fluid shear can induce osteogenic linage commitment in MSCs using the same parameters in this study (Stavenschi *et al.*, 2017; Stavenschi *et al.*, 2018a), indicating that Hh signalling may regulate osteogenesis in response to multiple forms of biophysical stimuli. Hence our data adds to the significance of Hh signalling in regulating MSC behaviour and demonstrates the importance of Hh in MSC mechanotransduction and loading-induced osteogenesis.

Gpr161 is novel mechanoresponsive GPCR required for loading-induced MSC differentiation. Gpr161 is an orphan GPCR (Mukhopadhyay *et al.*, 2013; Hwang *et al.*, 2018), however upon application of mechanical stimulation via OFS, an upregulation of *Gpr161* gene expression was found, therefore leading us to believe that Gpr161 may be mechanoresponsive. While the significance of this increase in Gpr161 is unclear, the removal

462 of *Gpr161* in MSCs results in an altered response to fluid shear in relation to cAMP signalling
463 and downstream osteogenic gene expression. Gsα and adenylyl cyclase complexes have been
464 long studied as a model for signal transduction (Chen *et al.*, 1997). Gsα stimulates AC's
465 resulting in increased cAMP levels and activating the protein kinase A (PKA)-dependent
466 gene transcription pathway (Wilson *et al.*, 2009). Previously, we demonstrated that OFS
467 activates an AC6-dependent cAMP pathway mediating early osteogenic gene expression
468 (Johnson *et al.*, 2018) and is required for loading-induced endosteal bone formation in a Lepr
469 specific manor *in vivo* (Riffault *et al.,* 2020), indicating that Gpr161, as a Gsα, may be acting
470 through AC6 to coordinate MSC osteogenesis. Interestingly, studies using knockout mouse
471 models found that deletion of Gsα in osterix expressing cells results in severe osteoporosis
472 with fractures at birth and an increase in bone marrow adipocytes (Wu *et al.*, 2011; Sinha *et*
473 *al.*, 2014). Furthermore, given the demonstrated role for Gpr161 in skeletal development
474 (Hwang *et al.*, 2018) and the importance of mechanics in developmental biology (Nowlan *et*
475 *al.*, 2007), Gpr161 may represent a novel mechanosensor in the mechanobiology of
476 development. We also demonstrate that Gpr161 is required for increases in Hh signalling
477 which is consistent with a Gsα-AC-cAMP mediated activation of PKA mechanism resulting
478 in trafficking of Smo into the cilium and the activation of Hh signalling (Wilson *et al.*, 2009;
479 Bachmann *et al.*, 2016). While our data points to a positive association between Gpr161 and
480 Hh signalling via cAMP, studies have presented conflicting results where Gpr161 acting as a
481 negative regulator of Hh (Mukhopadhyay *et al.*, 2013). While this discrepancy is currently
482 unclear and requires further analysis, our data convincingly demonstrates a critical role for
483 Gpr161 in MSC mechanotransduction. The identification of a regulatory GPCR in MSC
484 mechanotransduction opens this GPCR up as a future target for mechanotherapeutics.

Both Gpr161 and Hh mediated-MSC mechanotransduction require IFT88/primary cilium, highlighting two potentially new components of cilium-mediated mechanotransduction. The primary cilium is known to play an important role in MSC and bone mechanobiology *in vitro* and *in vivo* (Hoey *et al.*, 2012; Chen *et al.*, 2016) but the mechanisms by which the cilium coordinates this process are poorly understood. Mechanically activated signalling in hMSCs was shown to be primary cilia dependent, where ablation of the primary cilium resulted in loss of the fluid flow induced *COX2* and *BMP2* gene expression. Moreover, knockdown of *IFT88* did not have an effect on basal Hh levels, which is consistent with our data (Hoey et al., 2012). The identification of Gpr161 as a cilia-localised GPCR acting upstream of AC6 coordinating cAMP signalling and osteogenesis is an important step in the elucidation of the mechanism of cilium mechanotransduction and identifies a missing upstream mechanosensitive component that can activate AC6 likely via Gsα. The identification of a cilia-localised mechanosensitive GPCR may also aid in the explanation of recently identified calcium independent cilia-mechanosensing mechanisms (Malone *et al.*, 2007; Delling *et al.*, 2016). While it is well reported that Hh signalling is linked to the primary cilium in mammalian cells (Goetz *et al.*, 2009; Shao *et al.*, 2012; Bangs & Anderson, 2017), this study highlights the regulation of mechanically-induced Hh via primary cilia. Interestingly, we also demonstrate that this Hh signalling is dependent on Gpr161 and AC6, which we previously demonstrated was a critical component of cilium-mediated mechanotransduction. While a more complete picture of the components of cilia-mediated MSC mechanotransduction has been identified, it is still unclear how a biophysical stimulus is transduced via the cilium. Traditional models in the kidney epithelium and endothelium have demonstrated a bending of the ciliary axoneme under fluid flow which generates strain

508 along the membrane that is sufficient to open mechanosensitive ion channels. This ciliary
509 bending would occur in our system, but it is not known whether this is a driving force in
510 GPR161 activation. Moreover, as GPR161 is not specific to the cilium, the primary
511 mechanosensing event may occur on the plasma membrane, with the ciliary microdomain
512 acting as a signalling centre to regulate downstream Hh signalling. While this alternative
513 mechanism still highlights a prominent role for the cilium in MSC mechanotransduction,
514 further research is required to ascertain the exact location of the cilium in this mechanism.

515 There are a number of limitations that must be considered. Firstly, this study has
516 identified a novel role of Gpr161 in MSC mechanotransduction and indicated that this
517 mechanism may be mediated through the primary cilium. This conclusion is based on the
518 well-known defect in ciliogenesis following *Ift88* depletion, and spatial localisation of Gpr161
519 and AC6. However, *Ift88* is known to have non-ciliary roles and both Gpr161 and AC6 not
520 specifically localised to the ciliary microdomain. Therefore, further cilia specific analysis
521 will be required to fully detail the role of the cilium in this mechanotransduction mechanism.
522 Secondly, the proposed mechanism has been identified using *in vitro* approaches over short
523 time frames. While we validated this mechanism using multiple consistent readouts (cAMP,
524 Hh and Osteogenic gene expression), further work is required to analyse the impact of this
525 mechanism on MSC lineage commitment and skeletal physiology *in vivo*. Furthermore, this
526 study utilises the immortalised C3H10T1/2 murine mesenchymal stem cell line as a model of
527 primary human MSC behaviour. While C3H10T1/2 cells closely mimic hMSC behaviour in
528 terms of mechanosensitivity and multipotency, this cell line is originally derived from a
529 sarcoma and thus Hh signalling may be affected. Further work is therefore required to
530 validate this mechanotransduction mechanism in primary human MSCs. Despite these

limitations, we have delineated a novel molecular mechanism of MSC mechanotransduction which potentially occurs at the primary cilium, whereby a biophysical stimulus triggers a pathway involving Gpr161, AC6, cAMP, and Hh leading to osteogenesis. Given the known expression of these signalling components in many cell types known to mediate bone formation, such as osteoblasts and osteocytes, this mechanism may translate across the osteogenic lineage.

Competing interests

The authors declare no conflict of interest with the contents of this article.

Funding

The study was supported by a European Research Council (ERC) Starting Grant (#336882), Irish Research Council Government of Ireland Postgraduate Scholarship (GOIPG/2014/1463; to G.P.J.) and a Science Foundation Ireland ERC Support Grant SFI 13/ERC/L2864 and Frontiers for the Future grant SFI (19/FFP/6533) (to D.A.H.).

Author Contributions

G.P.J: Conception and design, Collection and/or assembly of data, Data analysis and interpretation, Manuscript writing,

S.F: Financial support, Approval of manuscript.

D.A.H: Conception and design, Data analysis and interpretation, Manuscript writing, Financial support, Final approval of manuscript.

551

552 **References**

553 Alcedo J, Zou Y & Noll M. (2000). Posttranscriptional regulation of smoothened is part of a self-
554 correcting mechanism in the Hedgehog signaling system. *Mol Cell* **6,** 457-465.

555

556 Bachmann VA, Mayrhofer JE, Ilouz R, Tschaikner P, Raffeiner P, Rock R, Courcelles M, Apelt F,
557 Lu TW, Baillie GS, Thibault P, Aanstad P, Stelzl U, Taylor SS & Stefan E. (2016). Gpr161
558 anchoring of PKA consolidates GPCR and cAMP signaling. *Proc Natl Acad Sci U S A* **113,**
559 7786-7791.

560

561 Bangs F & Anderson KV. (2017). Primary Cilia and Mammalian Hedgehog Signaling. *Cold Spring*
562 *Harb Perspect Biol* **9**.

563

564 Berbari NF, O'Connor AK, Haycraft CJ & Yoder BK. (2009). The Primary Cilium as a Complex
565 Signaling Center. *Current Biology* **19,** R526-R535.

566

567 Cai JQ, Huang YZ, Chen XH, Xie HL, Zhu HM, Tang L, Yang ZM, Huang YC & Deng L. (2012).
568 Sonic hedgehog enhances the proliferation and osteogenic differentiation of bone marrow-
569 derived mesenchymal stem cells. *Cell Biol Int* **36,** 349-355.

570

571 Chachisvilis M, Zhang YL & Frangos JA. (2006). G protein-coupled receptors sense fluid shear stress
572 in endothelial cells. *Proc Natl Acad Sci U S A* **103,** 15463-15468.

573

574 Chan CKF, Gulati GS, Sinha R, Tompkins JV, Lopez M, Carter AC, Ransom RC, Reinisch A, Wearda
575 T, Murphy M, Brewer RE, Koepke LS, Marecic O, Manjunath A, Seo EY, Leavitt T, Lu WJ,
576 Nguyen A, Conley SD, Salhotra A, Ambrosi TH, Borrelli MR, Siebel T, Chan K, Schallmoser
577 K, Seita J, Sahoo D, Goodnough H, Bishop J, Gardner M, Majeti R, Wan DC, Goodman S,
578 Weissman IL, Chang HY & Longaker MT. (2018). Identification of the Human Skeletal Stem
579 Cell. *Cell* **175,** 43-56 e21.

Chen JC, Hoey DA, Chua M, Bellon R & Jacobs CR. (2016). Mechanical signals promote osteogenic fate through a primary cilia-mediated mechanism. *Faseb Journal* **30,** 1504-1511.

Chen Q, Shou P, Zheng C, Jiang M, Cao G, Yang Q, Cao J, Xie N, Velletri T, Zhang X, Xu C, Zhang L, Yang H, Hou J, Wang Y & Shi Y. (2016c). Fate decision of mesenchymal stem cells: adipocytes or osteoblasts? *Cell Death Differ* **23,** 1128-1139.

Chen Y, Harry A, Li J, Smit MJ, Bai X, Magnusson R, Pieroni JP, Weng G & Iyengar R. (1997). Adenylyl cyclase 6 is selectively regulated by protein kinase A phosphorylation in a region involved in Galphas stimulation. *Proc Natl Acad Sci U S A* **94,** 14100-14104.

Corrigan MA, Ferradaes TM, Riffault M & Hoey DA. (2019). Ciliotherapy Treatments to Enhance Biochemically- and Biophysically-Induced Mesenchymal Stem Cell Osteogenesis: A Comparison Study. *Cell Mol Bioeng* **12,** 53-67.

Corrigan MA, Johnson GP, Stavenschi E, Riffault M, Labour MN & Hoey DA. (2018). TRPV4-mediates oscillatory fluid shear mechanotransduction in mesenchymal stem cells in part via the primary cilium. *Sci Rep* **8,** 3824.

Delling M, Indzhykulian AA, Liu X, Li Y, Xie T, Corey DP & Clapham DE. (2016). Primary cilia are not calcium-responsive mechanosensors. *Nature* **531,** 656-660.

Ehlen HW, Buelens LA & Vortkamp A. (2006). Hedgehog signaling in skeletal development. *Birth Defects Res C Embryo Today* **78,** 267-279.

Frost HM. (1963). Measurement of human bone formation by means of tetracycline labelling. *Can J Biochem Physiol* **41,** 31-42.

609 Goetz SC, Ocbina PJR & Anderson KV. (2009). The Primary Cilium as a Hedgehog Signal
610 Transduction Machine. *Primary Cilia* **94,** 199-+.

611

612 Hoey DA, Tormey S, Ramcharan S, O'Brien FJ & Jacobs CR. (2012). Primary cilia-mediated
613 mechanotransduction in human mesenchymal stem cells. *Stem Cells* **30,** 2561-2570.

614

615 Hwang SH, White KA, Somatilaka BN, Shelton JM, Richardson JA & Mukhopadhyay S. (2018). The
616 G protein-coupled receptor Gpr161 regulates forelimb formation, limb patterning and skeletal
617 morphogenesis in a primary cilium-dependent manner. *Development* **145**.

618

619 James AW, Pang S, Askarinam A, Corselli M, Zara JN, Goyal R, Chang L, Pan A, Shen J, Yuan W,
620 Stoker D, Zhang X, Adams JS, Ting K & Soo C. (2012). Additive effects of sonic hedgehog
621 and Nell-1 signaling in osteogenic versus adipogenic differentiation of human adipose-
622 derived stromal cells. *Stem Cells Dev* **21,** 2170-2178.

623

624 Johnson GP, Stavenschi E, Eichholz KF, Corrigan MA, Fair S & Hoey DA. (2018a). Mesenchymal
625 stem cell mechanotransduction is cAMP dependent and regulated by adenylyl cyclase 6 and
626 the primary cilium. *Journal of Cell Science*.

627

628 Kinto N, Iwamoto M, Enomoto-Iwamoto M, Noji S, Ohuchi H, Yoshioka H, Kataoka H, Wada Y,
629 Yuhao G, Takahashi HE, Yoshiki S & Yamaguchi A. (1997). Fibroblasts expressing Sonic
630 hedgehog induce osteoblast differentiation and ectopic bone formation. *FEBS Lett* **404,** 319-
631 323.

632

633 Knight MN & Hankenson KD. (2013). Mesenchymal Stem Cells in Bone Regeneration. *Adv Wound*
634 *Care (New Rochelle)* **2,** 306-316.

635

636 Labour MN, Riffault M, Christensen ST & Hoey DA. (2016). TGFbeta1 - induced recruitment of
637 human bone mesenchymal stem cells is mediated by the primary cilium in a SMAD3-
638 dependent manner. *Sci Rep* **6,** 35542.

Malone AM, Anderson CT, Tummala P, Kwon RY, Johnston TR, Stearns T & Jacobs CR. (2007). Primary cilia mediate mechanosensing in bone cells by a calcium-independent mechanism. *Proc Natl Acad Sci U S A* **104,** 13325-13330.

Matic I, Matthews BG, Wang X, Dyment NA, Worthley DL, Rowe DW, Grcevic D & Kalajzic I. (2016). Quiescent Bone Lining Cells Are a Major Source of Osteoblasts During Adulthood. *Stem Cells* **34,** 2930-2942.

Mukhopadhyay S, Wen X, Ratti N, Loktev A, Rangell L, Scales SJ & Jackson PK. (2013). The ciliary G-protein-coupled receptor Gpr161 negatively regulates the Sonic hedgehog pathway via cAMP signaling. *Cell* **152,** 210-223.

Nowlan NC, Murphy P & Prendergast PJ. (2007). Mechanobiology of embryonic limb development. *Ann N Y Acad Sci* **1101,** 389-411.

Park D, Spencer JA, Koh BI, Kobayashi T, Fujisaki J, Clemens TL, Lin CP, Kronenberg HM & Scadden DT. (2012). Endogenous bone marrow MSCs are dynamic, fate-restricted participants in bone maintenance and regeneration. *Cell Stem Cell* **10,** 259-272.

Pedersen, L. B. & Rosenbaum, J. L. 2008. Chapter Two Intraflagellar Transport (IFT): Role in Ciliary Assembly, Resorption and Signalling. *Current Topics in Developmental Biology,* 85**,** 23-61.

Rando TA & Ambrosio F. (2018). Regenerative Rehabilitation: Applied Biophysics Meets Stem Cell Therapeutics. *Cell Stem Cell* **22,** 306-309.

Riffault, M., Johnson, G.P., Owen, M.M., Javaheri, B., Pitsillides, A.A. and Hoey, D.A., 2020. Loss of Adenylyl Cyclase 6 in Leptin Receptor-Expressing Stromal Cells Attenuates Loading-Induced Endosteal Bone Formation. *JBMR plus*, *4*(11), p.e10408.

668
669 Ruiz-Perez VL, Blair HJ, Rodriguez-Andres ME, Blanco MJ, Wilson A, Liu YN, Miles C, Peters H
670 & Goodship JA. (2007). Evc is a positive mediator of Ihh-regulated bone growth that localises
671 at the base of chondrocyte cilia. *Development* **134,** 2903-2912.
672
673 Shao YY, Wang L, Welter JF & Ballock RT. (2012). Primary cilia modulate Ihh signal transduction
674 in response to hydrostatic loading of growth plate chondrocytes. *Bone* **50,** 79-84.
675
676 Shi Y, Chen J, Karner CM & Long F. (2015). Hedgehog signaling activates a positive feedback
677 mechanism involving insulin-like growth factors to induce osteoblast differentiation. *Proc*
678 *Natl Acad Sci U S A* **112,** 4678-4683.
679
680 Sinha P, Aarnisalo P, Chubb R, Ono N, Fulzele K, Selig M, Saeed H, Chen M, Weinstein LS, Pajevic
681 PD, Kronenberg HM & Wu JY. (2014). Loss of Gsalpha early in the osteoblast lineage favors
682 adipogenic differentiation of mesenchymal progenitors and committed osteoblast precursors.
683 *J Bone Miner Res* **29,** 2414-2426.
684
685 Spinella-Jaegle S, Rawadi G, Kawai S, Gallea S, Faucheu C, Mollat P, Courtois B, Bergaud B, Ramez
686 V, Blanchet AM, Adelman G, Baron R & Roman-Roman S. (2001a). Sonic hedgehog
687 increases the commitment of pluripotent mesenchymal cells into the osteoblastic lineage and
688 abolishes adipocytic differentiation. *Journal of Cell Science* **114,** 2085-2094.
689
690 Stavenschi E, Corrigan MA, Johnson GP, Riffault M & Hoey DA. (2018a). Physiological cyclic
691 hydrostatic pressure induces osteogenic lineage commitment of human bone marrow stem
692 cells: a systematic study. *Stem Cell Res Ther* **9,** 276.
693
694 Stavenschi E, Labour MN & Hoey DA. (2017). Oscillatory fluid flow induces the osteogenic lineage
695 commitment of mesenchymal stem cells: The effect of shear stress magnitude, frequency,
696 and duration. *J Biomech* **55,** 99-106.
697

698 Thompson CL, Chapple JP & Knight MM. (2014). Primary cilia disassembly down-regulates
699 mechanosensitive hedgehog signalling: a feedback mechanism controlling ADAMTS-5
700 expression in chondrocytes. *Osteoarthritis Cartilage* **22,** 490-498.

701

702 Tiecke E, Turner R, Sanz-Ezquerro JJ, Warner A & Tickle C. (2007). Manipulations of PKA in chick
703 limb development reveal roles in digit patterning including a positive role in Sonic Hedgehog
704 signaling. *Dev Biol* **305,** 312-324.

705

706 Vuolo L, Herrera A, Torroba B, Menendez A & Pons S. (2015). Ciliary adenylyl cyclases control the
707 Hedgehog pathway. *J Cell Sci* **128,** 2928-2937.

708

709 Wilson CW, Chen MH & Chuang PT. (2009). Smoothened adopts multiple active and inactive
710 conformations capable of trafficking to the primary cilium. *PLoS One* **4,** e5182.

711

712 Wu JY, Aarnisalo P, Bastepe M, Sinha P, Fulzele K, Selig MK, Chen M, Poulton IJ, Purton LE, Sims
713 NA, Weinstein LS & Kronenberg HM. (2011). Gsalpha enhances commitment of
714 mesenchymal progenitors to the osteoblast lineage but restrains osteoblast differentiation in
715 mice. *J Clin Invest* **121,** 3492-3504.

716

717 Xu J, Mathur J, Vessieres E, Hammack S, Nonomura K, Favre J, Grimaud L, Petrus M, Francisco A,
718 Li JY, Lee V, Xiang FL, Mainquist JK, Cahalan SM, Orth AP, Walker JR, Ma S, Lukacs V,
719 Bordone L, Bandell M, Laffitte B, Xu Y, Chien S, Henrion D & Patapoutian A. (2018).
720 GPR68 Senses Flow and Is Essential for Vascular Physiology. *Cell* **173,** 762-+.

721

722 **Figure legends**

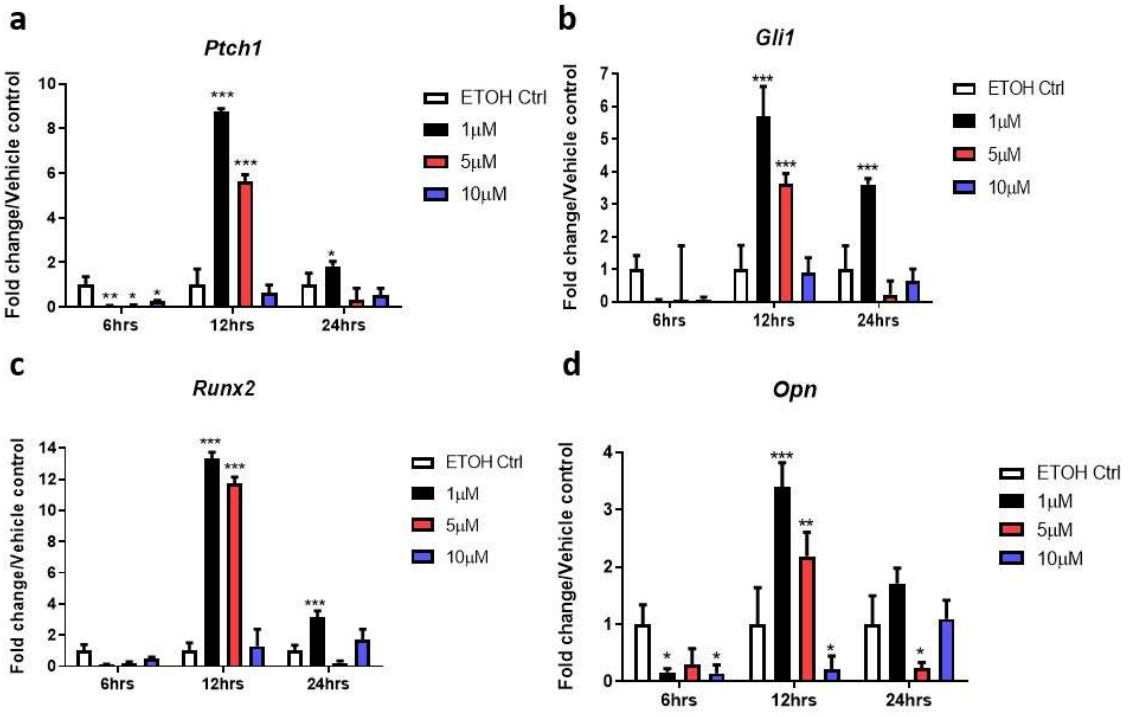

723

724 **Figure 1:** Relationship of hedgehog signalling in MSCs with osteogenic gene expression.
725 Dose and temporal effect of the hedgehog inhibitor cyclopamine of (A) *Ptch1*, (B) *Gli1*, (C)
726 *Runx2*, and (D) *Opn* gene expression (n=3). Statistical tests employed was a two-way
727 ANOVA with Bonferroni post-hoc. Values are means ± s.d. for three independent replicates.
728 **P*<0.05, ***P*<0.01, ****P*<0.001

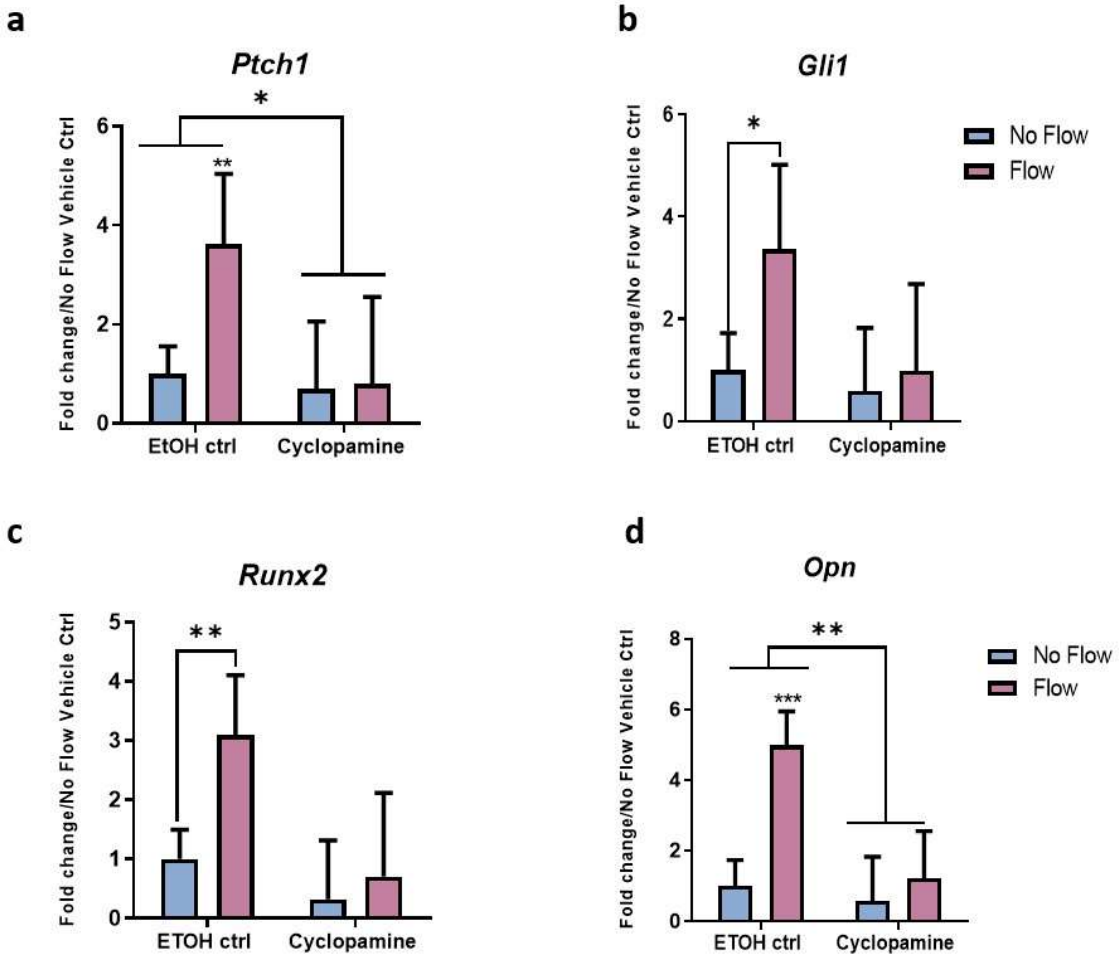

729

730 **Figure 2:** Hedgehog signalling is mechanoresponsive and required for fluid shear induced
731 hedgehog and osteogenic gene expression in MSCs. Effect of oscillatory fluid flow over cells
732 treated with 1μM cyclopamine at 1Pa, 1Hz on (A) *Ptch1*, (B) *Gli1*, (C) *Runx2* and (D) *Opn*
733 gene expression after 2 hours (N=2, n=6). Cells were treated with 1μM cyclopamine for 4
734 hours prior and during the 2 hours of flow. Statistical tests employed a two-way ANOVA with
735 Bonferroni post-hoc. Values are means ± s.d. **P*<0.05, ***P*<0.01 ****P*<0.001

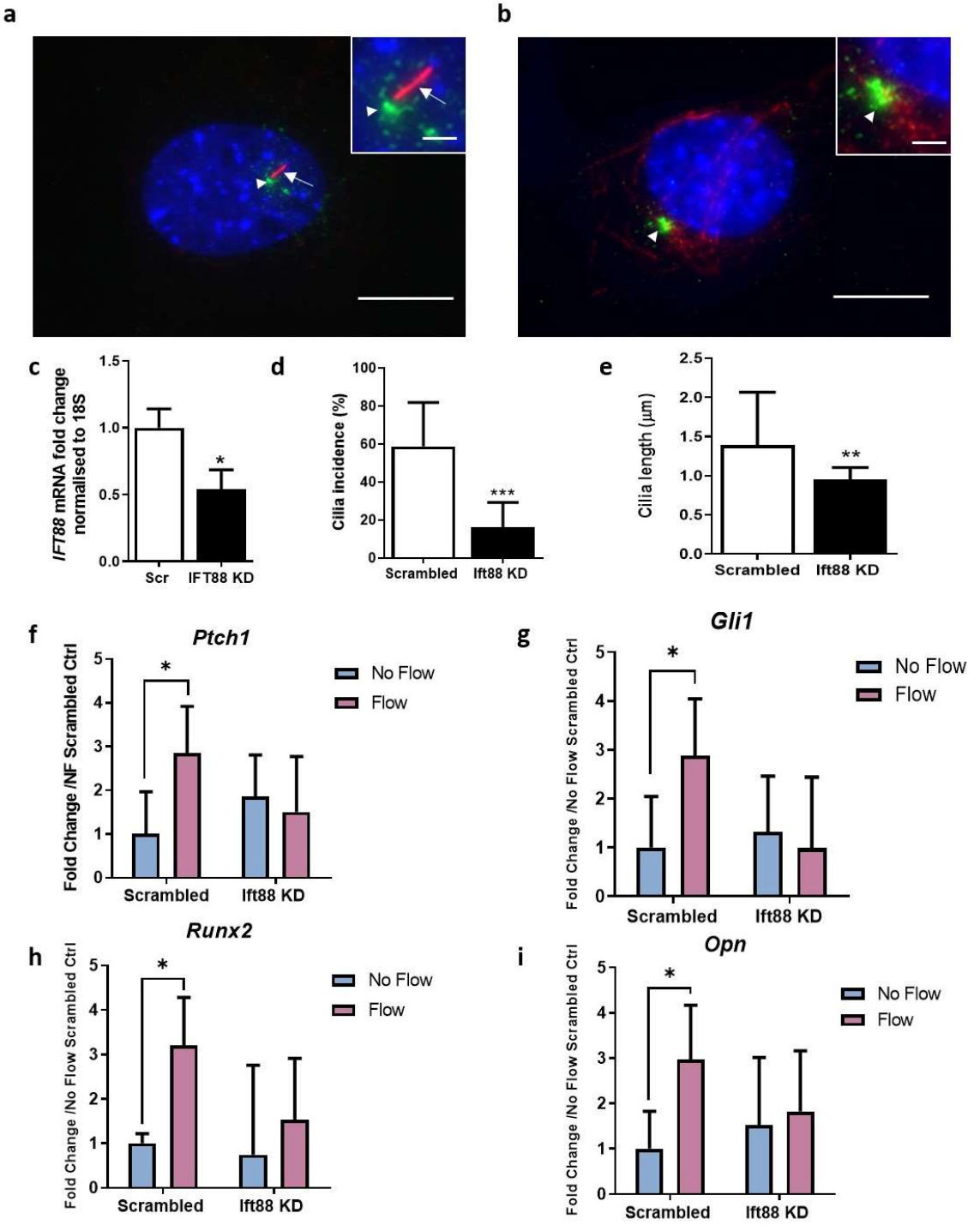

736

737 **Figure 3***: Ift88* is required for fluid shear induced hedgehog and osteogenic gene expression

738 in MSCs. (a-b) *Ift88* expression was successfully knocked down in MSCs using *Ift88* siRNA

739 as verified by immunostaining (a,b) and qRT-PCR (n=4; c). Cells were treated with either
740 scrambled siRNA (a) or *Ift88* siRNA (b) and stained for primary cilia, identified as linear
741 structures enriched in acetylated α-tubulin, (red; arrows) and centrioles (green; arrow head).
742 Nuclei are counterstained with DAPI (blue). Scale bars represent 10μm and 1μm (insert).
743 Effect of *Ift88* siRNA treatment on cilia incidence (N=4,n= 143-187; d). (f-i) Effect of
744 oscillatory fluid flow at 1Pa, 1Hz over cells treated with scrambled or *Ift88* siRNA on (f)
745 *Ptch1*, (g) *Gli1*, (h) *Runx2* and (i) *Opn* gene expression after 2 hrs (N=2, n=6). Statistical tests
746 employed a two-way ANOVA with Bonferroni post-hoc. Values are means ± s.d. *P<0.05,
747 **P<0.01, ***P<0.001

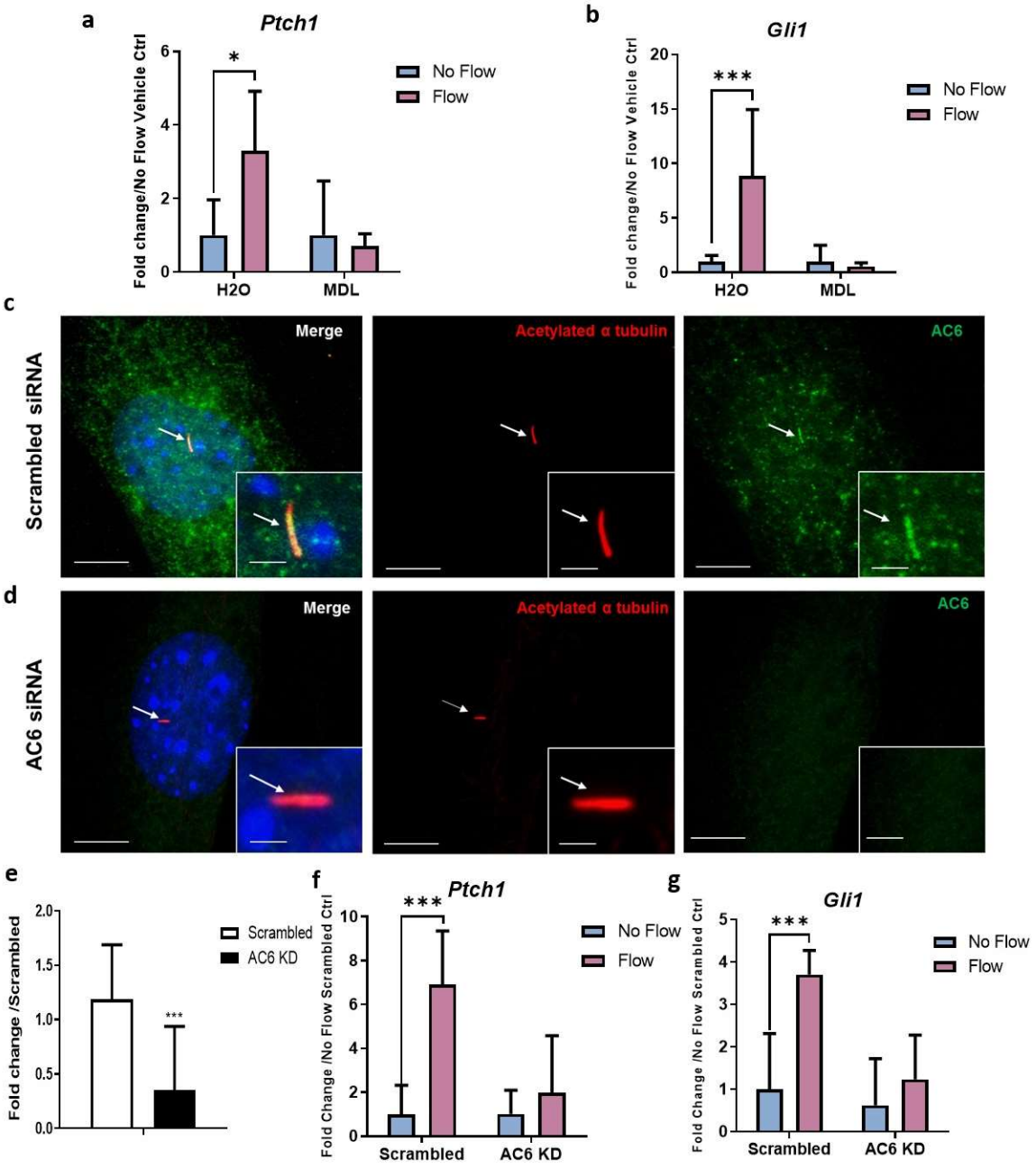

748

749 **Figure 4:** Adenylyl cyclases are required for fluid shear induced hedgehog gene expression
750 in MSCs. (A-B) Effect of MDL on (A) *Ptch1* and (B) *Gli1* gene expression following
751 oscillatory fluid flow at 1 Pa, 1 Hz for two hours (N=2, n=6). (C-D) Adenylyl Cyclase 6
752 expression was knocked down in MSCs using *Ac6* siRNA as verified by immunostaining (C-

753 D;N=3, n=50-77) and qPCR (E; N=4, n=12). Cells were treated with either scrambled siRNA
754 (C) or *Ac6* siRNA (D) and stained for primary cilia, identified as linear structures enriched
755 in acetylated α-tubulin, (red; arrows) and AC6 (green). Nuclei are counterstained with DAPI
756 (blue). Scale bars: 10μm and 1μm (insert). (F-G) Effect of oscillatory fluid flow at 1 Pa, 1 Hz
757 over cells treated with scrambled or *Ac6* siRNA on expression of hedgehog genes (F) *Ptch1*
758 and (G) *Gli1* after 2 hrs (N=4, n=9–12). Statistical tests employed a two-way ANOVA with
759 Bonferroni post-tests. Values are means ± s.d. **P*<0.05, ***P*<0.01 ****P*<0.001

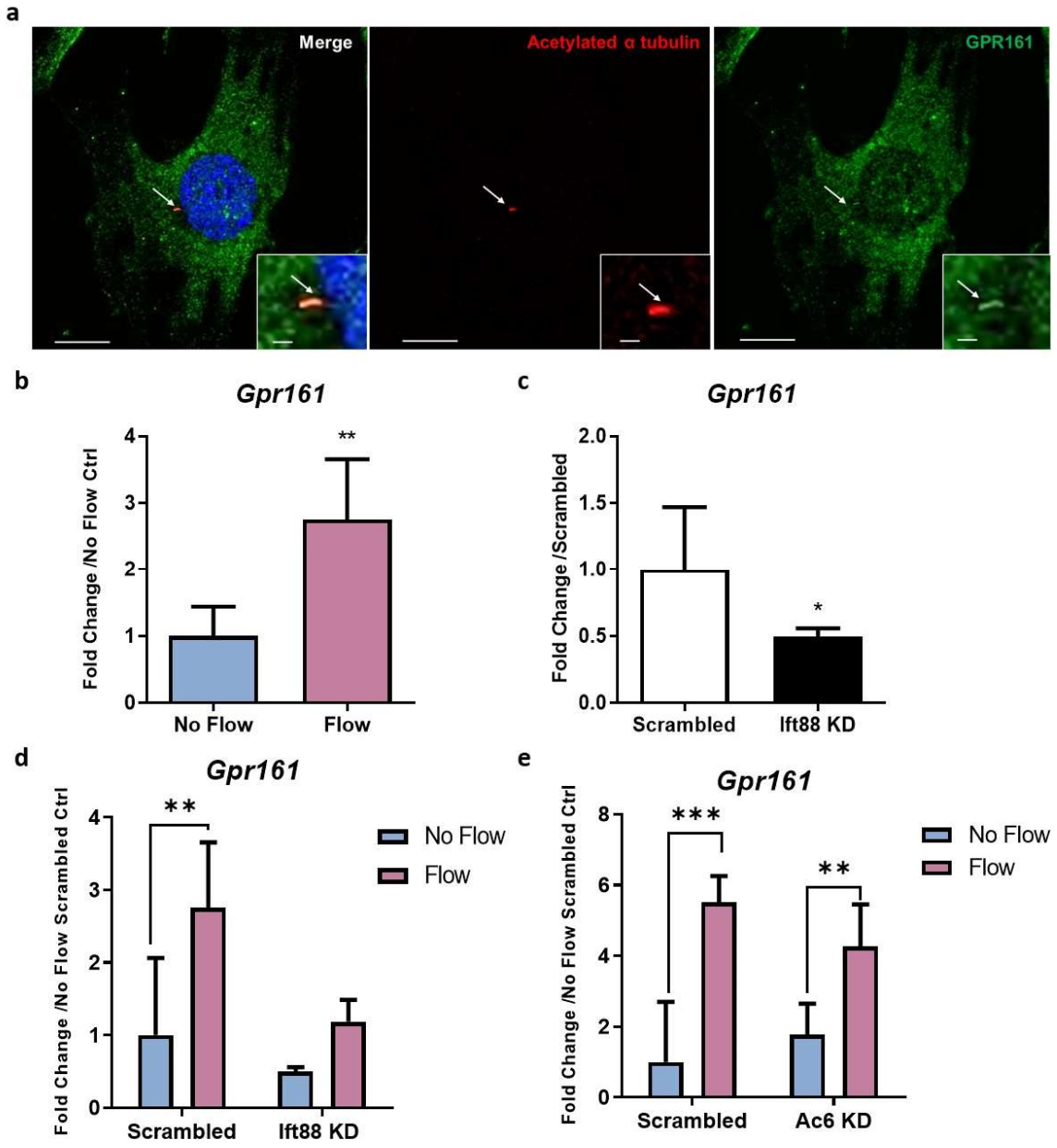

760

761 **Figure 5:** GPR161 is expressed in MSCs and localized to the primary cilium, where it is
762 mechanically regulated via primary cilia but not *Ac6*. (A) GPR161 (green) co-localisation to
763 the primary cilia, identified as linear structures enriched in acetylated α-tubulin (red; arrows).
764 Nuclei are counterstained with DAPI (blue). Scale bar: 10μm and 1μm (insert). (B) Effect of

765 oscillatory fluid flow at 1Pa, 1Hz on *Gpr161* gene expression after 2 hours. (C) Gene
766 expression of *Gpr161* following treatment with *Ift88* siRNA. (D) *Gpr161* gene expression
767 following fluid flow over cells treated with scrambled or *Ift88* siRNA. (E) Effect of fluid
768 flow on *Gpr161* expression over cells treated with scrambled or *Ac6* siRNA. (N=2, n=6).
769 Statistical test: unpaired two tailed student t-test with Wilcoxon correction (B-C) and a two-
770 way ANOVA with Bonferroni post-hoc (D-E). Values are means ± s.d. *P<0.05, **P<0.01,
771 ***P<0.001

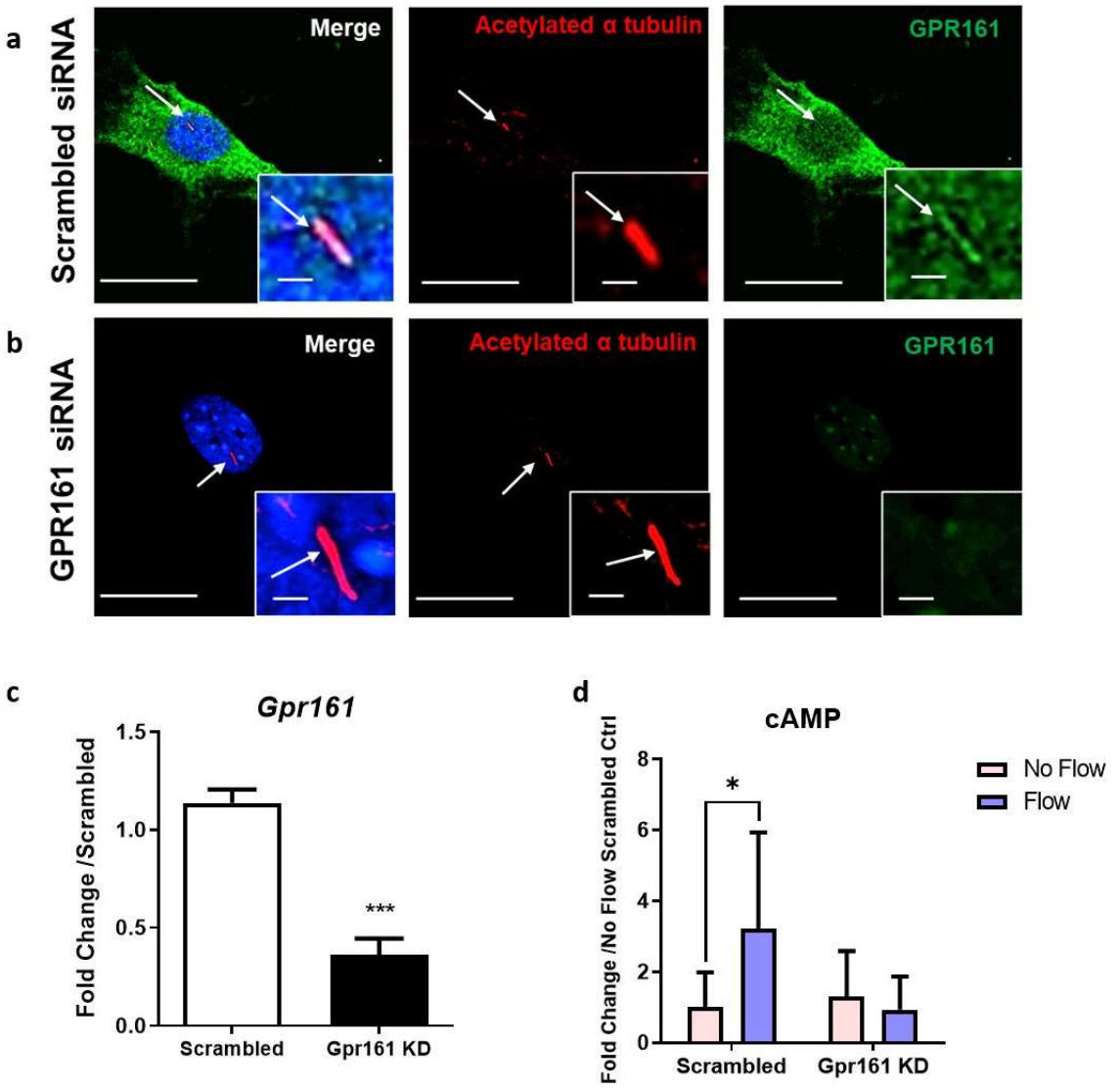

772

773 **Figure 6:** Gpr161 is required for fluid flow induced cAMP signalling and Hedgehog gene
774 expression in MSCs. (A-C) *Gpr161* expression was knocked down in MSCs using *Gpr161*
775 siRNA as verified by immunocytochemistry (A-B) and qRT-PCR (C, N=2, n=4). Cells were
776 treated with either scrambled siRNA (A) or *Gpr161* siRNA (B) and stained for primary cilia,
777 identified as linear structures enriched in acetylated α-tubulin, (red, arrows) and GPR161
778 (green). Nuclei are counterstained with DAPI (blue). Scale bars: 5 µm and 1 µm (insert). (D)

Effect of oscillatory fluid flow over MSCs treated with scrambled and *Gpr161* siRNA at 1 Pa, 1 Hz for 15 min on cAMP concentration (N=3, n=9). Statistical test: unpaired two tailed student t-test with Wilcoxon correction (C) and a two-way ANOVA with Bonferroni post-hoc (D-F). Values are means ± s.d. for a minimum of three independent replicates. **P*<0.05, ****P*<0.001.

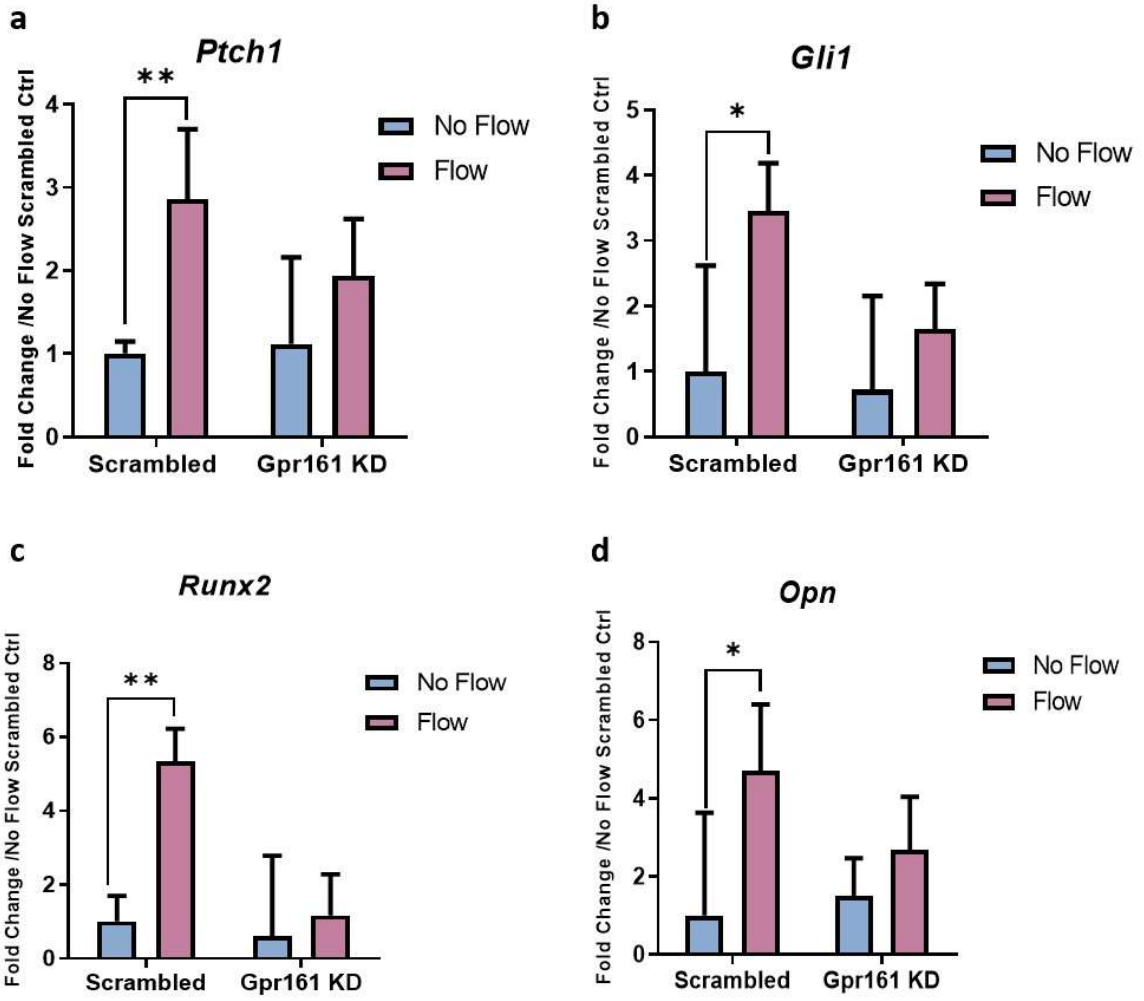

Figure 7: Fluid flow-induced increases in Hedgehog and Osteogenic signalling is dependent on Gpr161 in MSCs. Effect of oscillatory fluid flow at 1 Pa, 1 Hz over cells treated with

scrambled or *Gpr161* siRNA on expression of hedgehog genes *Ptch1* (A) and *Gli1* (B) after 2 hrs. Effect of oscillatory fluid flow at 1 Pa, 1 Hz on expression of osteogenic genes (C) *Runx2* and (D) *Opn* after 2 h (N=4, n=9–12), as determined by qRT-PCR. All groups are compared to no-flow scrambled control. Statistical test: two-way ANOVA with Bonferroni post-hoc. Values are means ± s.d. for a minimum of three independent replicates. **P*<0.05, ****P*<0.001.

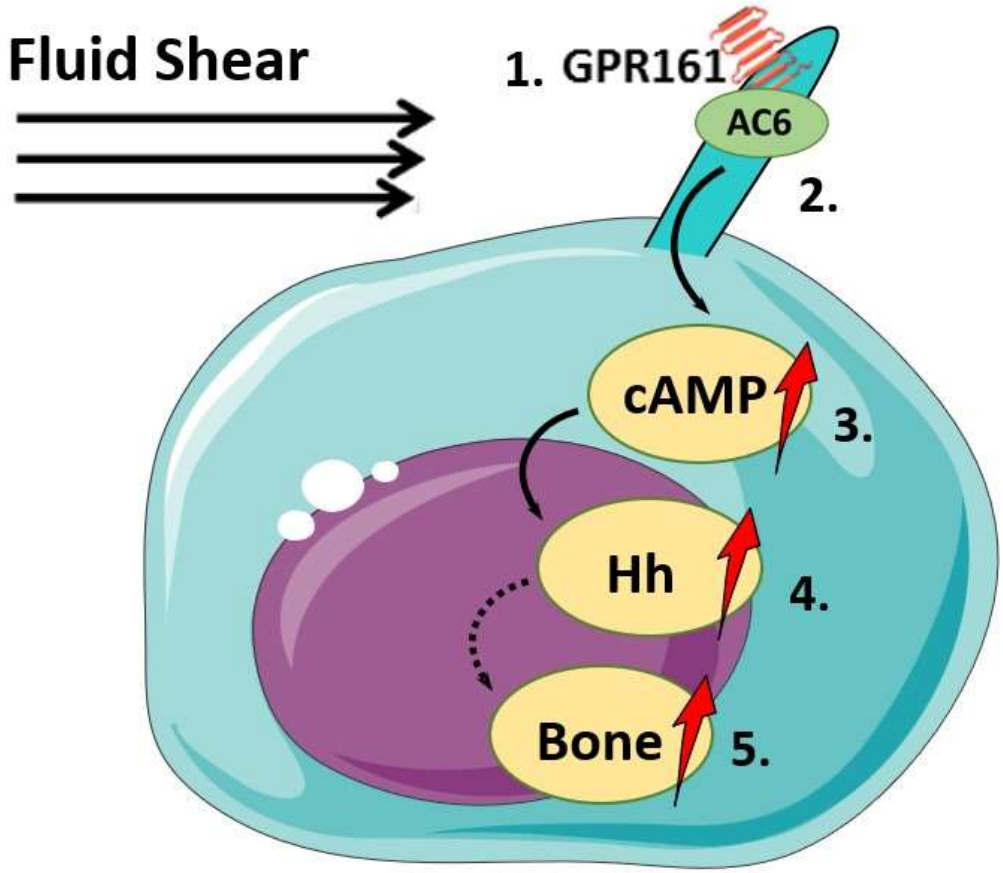

Figure 8: Schematic of proposed molecular mechanism of cilia mediated mechantoransduction in MSCs. (1-2) Fluid shear stimulates GPR161 at the primary cilium to activate AC6. (3-5) AC6 catalyzes the conversion of ATP into cAMP that stimulates an increase in the hedgehog genes *Ptch1* and *Gli1*, further resulting in the up regulation of

797 osteogenic gene expression. Solid arrow indicates established interaction in pathway. Dashed
798 arrow is suggested interaction.

799

800